

Characterization of Water Clusters in Organic Molecular Hosts from Density Functional Theory Calculations

Dominic R. Alfonso,^{*,†,¶} Karen Karapetian,[†] Dan C. Sorescu,[‡] and Kenneth D. Jordan^{*,†}

National Energy Technology Laboratory, Pittsburgh, Pennsylvania 15236, Parsons Project Services, Inc., South Park, Pennsylvania 15129, and Department of Chemistry and Center for Molecular and Materials Simulations, University of Pittsburgh, Pittsburgh, Pennsylvania 15260

Received: July 30, 2003; In Final Form: November 20, 2003

A density functional study of (H₂O)₆ and (H₂O)₈ clusters enclosed in organic hosts is undertaken. The calculations use supercells that contain up to 326 atoms. The crystal structures calculated for the (H₂O)₆/host and the (H₂O)₈/host systems are in qualitative agreement with those obtained from X-ray diffraction studies. The calculations confirm the presence of (H₂O)₈ clusters with C_i symmetry in the (H₂O)₈/host crystal and verify the existence of one-dimensional chains of fused water hexamers within channels of the (H₂O)₆/host crystal. The major differences observed between the calculated and experimental structures are attributed to the limitations of the Perdew–Wang functional for describing long-range dispersion interactions.

I. Introduction

Recently, huge strides have been made in the characterization of the low-energy isomers of small water clusters, with both theory and experiment making major contributions to our understanding of these species.^{1–12} For example, it is now well-established that (i) in isolation, the most stable isomers of the (H₂O)_n ($n = 3–5$) clusters have ring structures, (ii) (H₂O)₆ has a cagelike global minimum structure, and (iii) (H₂O)₈ has a cubiclike global minimum structure.^{5,7} Recently, several groups have reported the synthesis of organic or organometallic supramolecular systems with small water clusters or extended “chains” of water enclosed in cavities or channels.^{13–17} In the present study, we focus on two supramolecular systems that contain water: one with (H₂O)₈ clusters in cavities, and the other with extended chains of fused alternating six- and four-membered rings (where the ring size specifies the number of O atoms). We refer to the former as the “(H₂O)₈/host” system and the latter as the “(H₂O)₆/host” system.

The (H₂O)₈/host system has an [A₂B]·(H₂O)₈ composition, where A = κ^4 -[1,2-bis(2-oxy-methylpropan-amido)-4,5-dimethoxybenzene]cobaltate(III) and B = bis- κ^3 -[2,6-diacet-amidopyridine]cobalt(II).¹⁵ The organometallic host and the enclosed (H₂O)₈ cluster have C_i symmetry. This is particularly intriguing because the lowest energy minima of the isolated (H₂O)₈ cluster are D_{2d}- and S₄-symmetry “cubic” species, with the C_i-symmetry local minimum (which also has a “cubic” arrangement of the water monomers) lying ~2 kcal/mol higher in energy.⁵ This observation suggests that crystal hosts can be tailored so that various low-energy isomers of water clusters can be accessed.^{13,15,16,18} Finally, we note that, in a low-humidity environment, the water is irreversibly lost from the crystal, which causes the crystal structure to collapse.¹⁹

The (H₂O)₆/host system of ref 16 has a crystalline structure with chains of fused six-membered water rings along channels

formed by 2,4-dimethyl-5-aminobenzo[*b*]-1,8-naphthyridine ([C]) units. The water chains are coupled to N atoms (both in the aromatic rings and in amino groups) of the [C] groups through additional “bridging” water molecules.

Although some structural aspects of the (H₂O)₆/host and (H₂O)₈/host systems have been determined experimentally (by X-ray diffraction, XRD), important questions remain, in regard to the locations of the hydroxy H atoms and the extent to which the water clusters and chains are distorted by the hosts. The (H₂O)₈/host and (H₂O)₆/host systems are challenging systems to model theoretically, because current force fields are likely to be inadequate. This is particularly true for the former species, because it contains both divalent and trivalent cobalt. For this reason, we have decided to undertake a characterization of the crystal structures of the (H₂O)₆/host and (H₂O)₈/host with density functional theory (DFT), using a gradient-corrected electron-correlation functional. We recognize from the outset that this approach does not adequately describe dispersion interactions,²⁰ and that the success (or lack thereof) of the calculations will be dependent on the importance of such interactions in determining the crystal structures.

II. Methodology

The calculations were performed with the VASP²¹ code and used periodic supercells, ultrasoft pseudopotentials,²² and plane-wave basis sets. The Perdew–Wang (PW91) generalized gradient approximation (GGA),²³ which has been argued to provide a good description of hydrogen-bonded systems,²⁴ was used to calculate the exchange-correlation energy. The geometries of the periodic (H₂O)₆/host and (H₂O)₈/host systems were optimized both with the lattice parameters fixed to the experimental values and with relaxation of the lattice constants. The initial lattice parameters and initial positions of the atoms were taken from refs 15 and 16, which used XRD to determine the locations of the heavy atoms and refinement algorithms to locate the positions of the H atoms.

The supercells used for (H₂O)₆/host and (H₂O)₈/host contained 150 and 326 atoms, respectively. The crystals were generated by replicating the supercells by means of periodic boundary

* Author to whom correspondence should be addressed. E-mail: jordan@psc.edu.

[†] National Energy Technology Laboratory.

[‡] Parsons Project Services, Inc.

[¶] University of Pittsburgh.

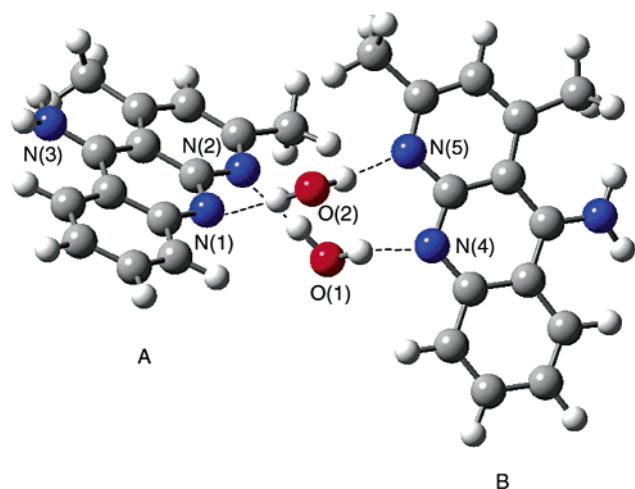


Figure 1. Two crystallographically independent benzonaphthyridine units (labeled by A and B) linked by water molecules. Only the “bridging” water molecules are shown. Colors are as follows: gray, carbon; red, oxygen; dark blue, nitrogen; and white, hydrogen. Hydrogen bonds are indicated by dashed lines.

conditions. Only the valence electrons were treated explicitly, with the nonvalence cores being modeled by ultrasoft pseudo-potentials.²² Γ -point sampling of the Brillouin zone was applied. The energy cutoff of the plane wave expansion was chosen to be 396 eV. Comparison with the results of calculations with lower-energy cutoffs indicates that the geometries and lattice constants should be relatively insensitive to further expansion of the basis set. The demands of the computer processing unit (CPU) and the large memory requirements of these calculations necessitated the use of an efficient parallel computer. To this end, the calculations were performed using 40–60 processors on the Terascale supercomputer at the Pittsburgh Supercomputer Center.

III. Results

A. $(\text{H}_2\text{O})_6/\text{Host}$. The crystal structure of the $(\text{H}_2\text{O})_6/\text{host}$ system consists of crystallographically independent 2,4-dimethyl-5-aminobenzo[*b*]-1,8-naphthyridine units linked together by the water network. Specifically, two benzonaphthyridine units in the same “sheet” are linked by two “bridging” water monomers through H-bonds to the ring N atoms (see Figure 1). In addition, each of these bridging water molecules acts as an H-bond acceptor for the amino group of a benzonaphthyridine molecule in an adjacent sheet (Figure 2). This results in stacks of benzonaphthyridine units with channels that are occupied by extended chains of fused six-membered water rings, as shown

in Figure 3. (The H-bonding between the six-membered rings results in alternating six- and four-membered rings.) Finally, water molecules of the chains also form H-bonds (acting as donors) to the bridging water molecules, as shown in Figure 4.

The crystal structure showing the lattice vectors is depicted in Figure 5. The calculations (both with and without optimization of the lattice constants) give a structure that is qualitatively consistent with that determined in the XRD measurements. Specifically, the channels contain extended chains with alternating six-membered and four-membered rings of water molecules, with the hexamers adopting chairlike conformations. The calculations, which allow for optimization of the lattice, give lattice constants *b* and *c* within 1% of the experimental X-ray values.¹⁶ However, the constant resulting *a* is $\sim 12\%$ larger than the experimental value. The α , β , and γ angles that define the unit cell are underestimated by -0.5% , -4% , and -3% , respectively, and the corresponding cell volume is overestimated by $\sim 9\%$.²⁵

Selected computed internal geometric parameters are tabulated in Table 1. For the fully relaxed structure, the O(4)–O(3) and O(3)–O(5) distances in the water hexamer units are 0.13–0.17 Å greater than the experimentally observed values, whereas the calculated O(5)–O(4A) distance is ~ 0.04 Å smaller than the measured value. O(5)–H \cdots O(4) and O(5A)–H \cdots O(4A) correspond to the H-bonds at the juncture of fused six- and four-membered rings, and O(3)–H \cdots O(5), O(3A)–H \cdots O(5A), O(4)–H \cdots O(3), and O(4A)–H \cdots O(3A) correspond to the other four H-bonds in the hexamer units.

In the optimizations with the lattice constants fixed at the experimental values, the various nearest-neighbor O \cdots O distances are predicted to be similar to (i.e., within 0.04 Å) the experimentally determined values. However, imposition of the constraints causes large errors in some of the O \cdots O \cdots O angles, in particular, giving an O(3) \cdots O(5) \cdots O(4A) angle 11.3° larger and an O(5A) \cdots O(4) \cdots O(3) angle 7.1° smaller than the corresponding experimental values.

The measured O \cdots O distances for the $(\text{H}_2\text{O})_6/\text{host}$ system range from 2.71 Å to 2.83 Å, as compared to the 2.759 Å value in ice I_h , which is comprised of fused six-membered water rings.²⁶ The O \cdots O \cdots O angles in the $(\text{H}_2\text{O})_6/\text{host}$ system are 96.0° , 113.2° , and 140.0° , whereas in ice I_h , all these angles are 109.3° .²⁶ Thus, the $(\text{H}_2\text{O})_6$ rings in the $(\text{H}_2\text{O})_6/\text{host}$ system are appreciably distorted from those in ice I_h .

The PW91 optimized structure of the $(\text{H}_2\text{O})_6/\text{host}$ system has more nearly “planar” water hexamers than found experimentally, with the calculated O \cdots O \cdots O torsion angles being $\sim 60^\circ$ larger than experimental results. (The corresponding dihedral angles calculated with the constrained lattice constants are 5° –

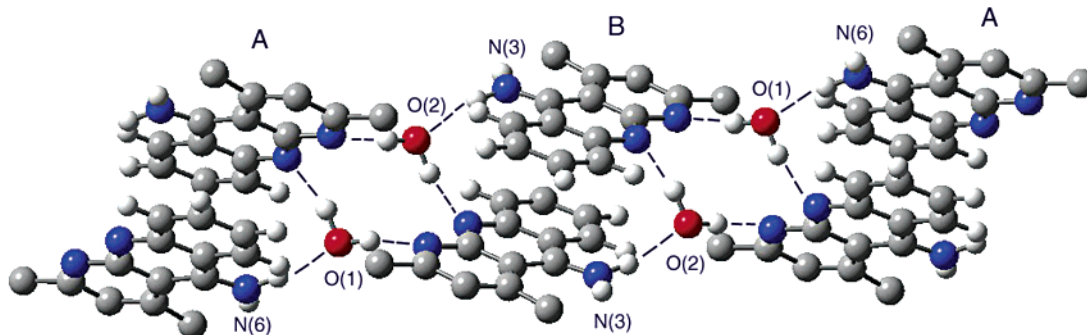


Figure 2. One-dimensional chain of hydrogen-bonded benzonaphthyridine dimers. The crystallographically independent benzonaphthyridine units are labeled by A and B. Only the bridging water molecules are shown. The methyl groups of the benzonaphthyridine units have been suppressed for clarity. Colors are as follows: gray, carbon; red, oxygen; dark blue, nitrogen; and white, hydrogen. Hydrogen bonds are indicated by dashed lines.

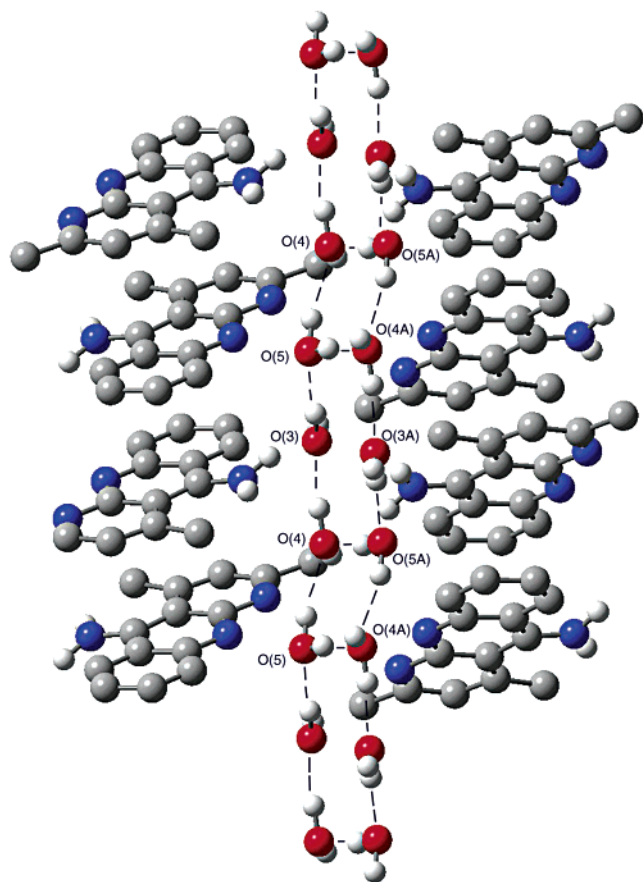


Figure 3. Section of the C-unit channel of the $(\text{H}_2\text{O})_6/\text{host}$ crystal structure containing a one-dimensional chainlike structure of cyclic water hexamer units. Colors are as follows: gray, carbon; red, oxygen; dark blue, nitrogen; and white, hydrogen. Hydrogen bonds are indicated by dashed lines. The water molecules that link the benzonaphthyridine units and some of the H atoms in the benzonaphthyridine units are omitted for clarity.

6° larger still.) Consistent with these results, both the calculated interhexamer $\text{O}(5\text{A})\cdots\text{O}(4\text{A})$ and $\text{O}(4)\cdots\text{O}(5)$ (see Figure 3) distances, and the spacing between the adjacent aromatic rings along the channels, are $\sim 0.3 \text{ \AA}$ greater than the corresponding experimental distances. These results suggest that there are long-range interactions in the $(\text{H}_2\text{O})_6/\text{host}$ system that are not properly

described by the DFT–PW91 calculations. We believe that this is a reflection of the inadequacy of the PW91 method for describing dispersion interactions.

To gain more insight into the origin of the deficiencies of the DFT–PW91 approach for describing the $(\text{H}_2\text{O})_6/\text{host}$ system, the geometry of an isolated $(\text{H}_2\text{O})_6$ cluster with the ring structure was optimized using the PW91 method with Gaussian-orbital, as well as plane-wave, basis sets. The Gaussian-orbital calculations made use of the aug-cc-pVDZ Gaussian orbital basis set,²⁷ and the plane-wave calculations used ultrasoft pseudopotentials, an energy cutoff of 495.0 eV, and a $15 \text{ \AA} \times 15 \text{ \AA} \times 15 \text{ \AA}$ cell. The resulting geometrical parameters are compared in Table 2 with those from an MP2 optimization that also used the aug-cc-pVDZ basis set.²⁸ (The calculations with the Gaussian basis sets were performed using the Gaussian 03 program.²⁹) MP2/aug-cc-pVDZ calculations are expected to provide geometries that are in close agreement with experimental results for H-bonded systems. The PW91 calculations with the Gaussian and plane-wave basis sets give almost the same geometrical parameters for the isolated ringlike isomer of $(\text{H}_2\text{O})_6$, and, overall, there is fairly good agreement between the geometrical parameters obtained from the PW91 and MP2 optimizations. This lends credence to the interpretation that the deficiency of the PW91 procedure for describing the $(\text{H}_2\text{O})_6/\text{host}$ system results primarily from an inadequate description of the dispersion interactions between the aromatic rings (and, perhaps also, between the water molecules and the aromatic rings). To test this hypothesis, we performed PW91 and localized-orbital MP2 (LMP2)^{30,31} calculations on a system comprised of two adjacent “stacked” aromatic rings of the $(\text{H}_2\text{O})_6/\text{host}$ system, with the atomic coordinates being taken from the PW91 slab-model calculations. The LMP2 calculations give a much greater attraction (by $\sim 10.8 \text{ kcal/mol}$) between the aromatic rings than do the PW91 calculations. The LMP2 calculations include dispersion interactions; therefore, we conclude that a significant source of error in the PW91 optimized geometry of the $(\text{H}_2\text{O})_6/\text{host}$ system is the failure to describe the dispersion interactions between the aromatic rings.

B. $(\text{H}_2\text{O})_8/\text{Host}$. The $(\text{H}_2\text{O})_8/\text{host}$ crystal possesses well-defined channels that open into cavities, surrounded by four $[\text{A}]^-$ units, which, in turn, are linked to two $[\text{B}]^{+2}$ units. Each cavity contains a “cubic” $(\text{H}_2\text{O})_8$ cluster anchored to the host by four H-bonds from the cube to the OH groups of the $[\text{A}]^-$

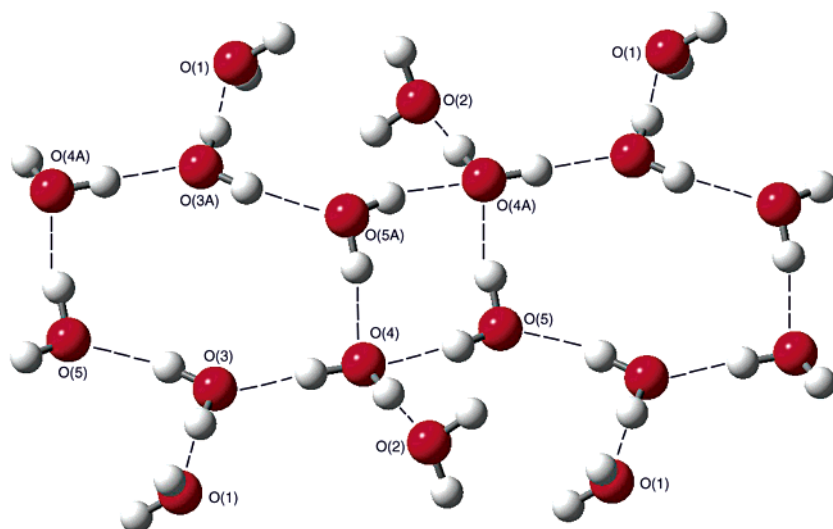


Figure 4. Section of a one-dimensional chain of water hexamers in the $(\text{H}_2\text{O})_6/\text{host}$ system. Hydrogen bonds are indicated by dashed lines. Bridging water molecules, denoted by O(1) and O(2), anchor the water chain to the organic framework.

TABLE 1: Comparison of Calculated and Experimental Structural Parameters for Cyclic (H₂O)₆ in the (H₂O)₆/Host Crystal^a

hydrogen bond identification	$r(\text{O}-\text{H})$ (Å)	$r(\text{O}\cdots\text{O})$ (Å)		$r(\text{H}\cdots\text{O})$ (Å)	$\theta(\text{O}-\text{H}\cdots\text{O})$ (deg)
	calc	calc	expt	calc	calc
O(4)-H \cdots O(3)	0.992 (1.001)	2.839 (2.712)	2.711	1.853 (1.715)	172.4 (173.1)
O(3)-H \cdots O(5)	0.987 (0.995)	2.958 (2.770)	2.785	1.983 (1.783)	169.2 (170.8)
O(5)-H \cdots O(4A)	0.994 (0.990)	2.797 (2.796)	2.833	1.808 (1.808)	172.8 (174.9)
<hr/>					
OOO angle	$\theta(\text{O}\cdots\text{O}\cdots\text{O})$ (deg)		OOOO dihedral angle	$\theta(\text{O}\cdots\text{O}\cdots\text{O}\cdots\text{O})$ (deg)	
	calc	expt		calc	expt
O(3) \cdots O(5) \cdots O(4A)	115.8 (124.5)	113.2	O(5) \cdots O(3) \cdots O(4) \cdots O(3A)	158.3 (164.6)	106.2
O(5A) \cdots O(4) \cdots O(3)	94.2 (88.9)	96.0	O(5) \cdots O(4A) \cdots O(3A) \cdots O(4)	166.2 (170.8)	105.9
O(4) \cdots O(3) \cdots O(5)	142.6 (142.7)	140.2			

^a The calculated results were obtained using the DFT-PW91 method with periodic boundary conditions as described in the text, and the experimental results are from the X-ray studies of ref 16. Parameters optimized with the lattice constants constrained to their experimental values are reported in parentheses.

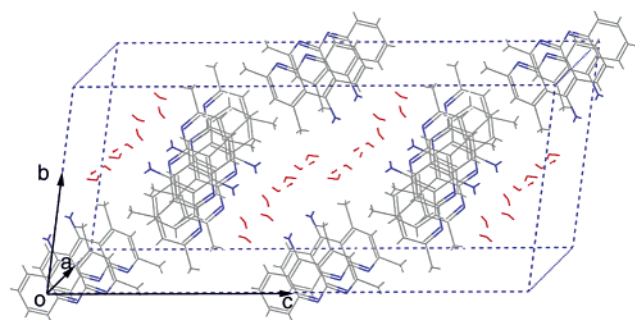


Figure 5. Section of the crystal structure of (H₂O)₆/host system showing the *a*-, *b*-, and *c*-axes. Angles α , β , and γ refer to angles between the *c*- and *b*-axes, the *a*- and *c*-axes, and the *a*- and *b*-axes, respectively.

TABLE 2: Comparison of the PW91 and MP2 Optimized Geometries of the Ring Form of an Isolated (H₂O)₆ Cluster

parameter	PW91 ^a	MP2 ^b
$r(\text{O}-\text{H})$ (Å)	0.971 (0.972)	0.961
$r(\text{O}(4)\cdots\text{O}(3))$ (Å)	2.651 (2.642)	2.707
$r(\text{H}\cdots\text{O})$ (Å)	1.644 (1.632)	1.723
$\theta(\text{O}(4)\cdots\text{H}\cdots\text{O}(3))$ (deg)	177.8 (179.0)	179.2
$\theta(\text{O}(3)\cdots\text{O}(5)\cdots\text{O}(4A))$ (deg)	119.4 (118.6)	118.8
$\theta(\text{O}(5)\cdots\text{O}(3)\cdots\text{O}(4)\cdots\text{O}(3A))$ (deg)	172.2 (168.2)	169.2

^a Two sets of PW91 results are reported. The first entry in each case was obtained using the aug-cc-pVDZ Gaussian basis set, and the second entry (in parentheses) was obtained using a plane-wave basis set. ^b MP2 geometry from ref 28.

units. The (H₂O)₈ cluster and the neighboring [A]⁻ units are depicted in Figure 6. The corresponding crystal structure, showing the lattice vectors, is displayed in Figure 7.

The DFT-PW91 calculations give a crystal structure with extended channels opening into cavities that contain (H₂O)₈ “cubes” of *C_i* symmetry, which is consistent with experimental results (see Figure 8). The computed cell volume agrees with that determined experimentally, to within 0.2%. However, the calculated values of the lattice constants *a* and γ differ from the experimental results by 6.0% and -4.8%, respectively.³²

The optimized geometrical parameters of the (H₂O)₈/host system are compared with the experimental values in Table 3. The calculated O \cdots O distances are 0.10–0.18 Å smaller than the experimentally measured values and the calculated O \cdots O \cdots O angles range from being 5.5° less than to being 6.8° greater than the corresponding experimental values. Table 3 also reports geometrical parameters for the (H₂O)₈/host system obtained from an optimization with the lattice parameters constrained to their experimental values. Comparison of the parameters from the constrained and unconstrained optimizations

to those of the experimentally determined structure reveals that the unconstrained optimization gives a structure for the enclosed (H₂O)₈ “cubes” that is more similar to that determined experimentally.

The calculations confirm that the water octamer is anchored to the organic framework by four H-bonds from water molecules in the octamer to O atoms in the organic molecules (see Figure 8). Two of the four “free” H atoms of (H₂O)₈ interact with the [A]⁻ methoxy O atoms with calculated O \cdots O distances of 2.785 Å, and O-H \cdots O angles of 146.3°. The X-ray measurements give a value of 2.897 Å for these O \cdots O distances. The other two “free” H atoms of the (H₂O)₈ cluster interact with the two framework [A]⁻ alkoxide O atoms. These O \cdots O bonds are also shorter than the measured values (2.600 Å (calculated) versus 2.788 Å (experimental)). The O-H \cdots O angles that involve these atoms are calculated to be 174.2°.

Table 4 reports geometrical parameters for an isolated (H₂O)₈ cluster with *C_i* symmetry optimized at the PW91/plane-wave, PW91/aug-cc-pVDZ, and MP2/aug-cc-pVDZ levels of theory. The plane-wave calculations used ultrasoft pseudopotentials, an energy cutoff of 495.0 eV, and a 15 Å \times 15 Å \times 15 Å cell. Again, the geometrical parameters from the two PW91 calculations are very similar, and, overall, good agreement exists between the PW91 and MP2 optimized structures, with the PW91 values of the O \cdots O separations being \sim 0.05–0.08 Å longer in the MP2 calculations. The agreement between the PW91 and MP2 structures for the isolated (H₂O)₈ complex is much better than that between the PW91 and experimental structures for the (H₂O)₈/host system. As for the (H₂O)₆/host system, this may reflect the importance of long-range dispersion interactions that are not recovered in the PW91 calculations.

It is also instructive to compare the MP2-optimized structure of the isolated *C_i* (H₂O)₈ cube and the experimental structure of the (H₂O)₈ in the (H₂O)₈/host system. Of the six symmetry-unique O-H \cdots O “bonds” in the *C_i* (H₂O)₈ cube, four have almost the same bond length in the (H₂O)₈/host system (experiment) as in the isolated cluster (MP2 level). However, the O(2)-H \cdots O(3) and O(3)-H \cdots O(4) distances are \sim 0.1 Å longer in the crystal than in the isolated cluster. Presumably, this is due to distortions that result from the H-bonding to the host.

IV. Conclusion

DFT calculations with the Perdew-Wang PW91 functional and periodic boundary conditions have been used to optimize the geometries of two water/host crystal systems. Overall, the structures predicted for the (H₂O)₆/host and (H₂O)₈/host systems are in qualitative agreement with the results of X-ray studies.

TABLE 3: Comparison of the Calculated and Experimental Structural Parameters of the (H₂O)₈ Cluster in the (H₂O)₈/Host Crystal^a

hydrogen bond identification	$r(\text{O}-\text{H})$ (Å)	$r(\text{O}\cdots\text{O})$ (Å)		$r(\text{H}\cdots\text{O})$ (Å)	$\theta(\text{O}-\text{H}\cdots\text{O})$ (deg)
	calc	calc	expt	calc	calc
O(1)–H \cdots O(2)	0.999 (1.004)	2.748 (2.690)	2.871	1.757 (1.691)	171.0 (172.3)
O(4)–H \cdots O(1)	1.008 (1.004)	2.689 (2.721)	2.784	1.704 (1.747)	164.5 (162.7)
O(2)–H \cdots O(3)	0.996 (0.995)	2.682 (2.695)	2.838	1.706 (1.712)	165.5 (168.9)
O(4')–H \cdots O(2)	0.995 (1.000)	2.724 (2.668)	2.903	1.759 (1.709)	162.2 (159.4)
O(3)–H \cdots O(4)	1.027 (1.027)	2.598 (2.586)	2.750	1.578 (1.568)	171.6 (170.0)
O(1')–H \cdots O(3)	0.991 (0.987)	2.795 (2.830)	2.929	1.844 (1.903)	160.0 (155.4)
O(3)–H \cdots O(5)	0.980 (0.978)	2.785 (2.807)	2.897	1.916 (1.929)	146.3 (148.0)
O(2)–H \cdots O(6)	1.012 (1.017)	2.600 (2.520)	2.788	1.591 (1.514)	174.2 (168.9)

OOO angle identification	$\theta(\text{O}\cdots\text{O}\cdots\text{O})$ (deg)		OOO angle identification	$\theta(\text{O}\cdots\text{O}\cdots\text{O})$ (deg)	
	calc	expt		calc	expt
O(1) \cdots O(2) \cdots O(3)	89.4 (94.3)	86.9	O(3) \cdots O(2) \cdots O(4')	95.2 (102.5)	88.4
O(1) \cdots O(4) \cdots O(3)	92.5 (96.1)	90.4	O(4) \cdots O(3) \cdots O(1')	88.0 (91.7)	81.5
O(1) \cdots O(2) \cdots O(4')	86.5 (93.1)	79.9	O(1) \cdots O(2) \cdots O(6)	109.2 (101.5)	120.6
O(2) \cdots O(3) \cdots O(4)	90.7 (85.9)	92.1	O(2) \cdots O(3) \cdots O(5)	168.5 (164.7)	169.3
O(2) \cdots O(3) \cdots O(1')	85.0 (78.6)	90.5	O(3) \cdots O(2) \cdots O(6)	109.5 (97.6)	114.2
O(2) \cdots O(1) \cdots O(4)	87.4 (83.4)	90.7			

^a The calculated results are from DFT–PW91 calculations, using periodic boundary conditions as described in the text, and the experimental results are from the X-ray studies of ref 15. Geometrical parameters optimized with the lattice constants constrained to their experimental values are reported in parentheses.

TABLE 4: Comparison of PW91 and MP2 Optimized Geometries of an Isolated C_{3v}-Symmetry (H₂O)₈ Cluster^a

hydrogen bond identification	$r(\text{O}-\text{H})$ (Å)		$r(\text{O}\cdots\text{O})$ (Å)		$r(\text{H}\cdots\text{O})$ (Å)		$\theta(\text{O}-\text{H}\cdots\text{O})$ (deg)	
	PW91	MP2	PW91	MP2	PW91	MP2	PW91	MP2
O(1)–H \cdots O(2)	0.985 (0.986)	0.974	2.876 (2.859)	2.913	1.931 (1.920)	1.978	159.8 (158.3)	160.0
O(4)–H \cdots O(1)	1.004 (1.006)	0.986	2.722 (2.706)	2.773	1.735 (1.719)	1.808	166.6 (166.0)	165.5
O(2)–H \cdots O(3)	1.003 (1.005)	0.985	2.690 (2.672)	2.755	1.715 (1.693)	1.799	162.9 (163.3)	162.9
O(4')–H \cdots O(2)	0.987 (0.988)	0.975	2.843 (2.826)	2.882	1.896 (1.877)	1.946	160.1 (159.9)	160.1
O(3)–H \cdots O(4)	1.034 (1.040)	1.003	2.582 (2.558)	2.640	1.556 (1.525)	1.649	170.5 (171.0)	169.1
O(1')–H \cdots O(3)	0.987 (0.988)	0.975	2.854 (2.843)	2.897	1.906 (1.898)	1.961	160.2 (159.3)	160.3

OOO angle	$\theta(\text{O}\cdots\text{O}\cdots\text{O})$ (deg)	
	PW91	MP2
O(1) \cdots O(2) \cdots O(3)	87.6 (87.4)	88.1
O(1) \cdots O(4) \cdots O(3)	93.2 (93.1)	93.5
O(1) \cdots O(2) \cdots O(4')	84.8 (85.1)	82.4
O(2) \cdots O(3) \cdots O(4)	93.0 (93.3)	92.2
O(2) \cdots O(3) \cdots O(1')	90.6 (92.7)	89.3
O(2) \cdots O(1) \cdots O(4)	86.2 (86.2)	86.2
O(3) \cdots O(2) \cdots O(4')	89.7 (87.7)	90.8
O(4) \cdots O(3) \cdots O(1')	90.2 (90.7)	87.0

^a Two sets of PW91 results are reported, the first entry in each case was obtained using the aug-cc-pVDZ basis set and the second entry (in parentheses) using a plane-wave basis set.

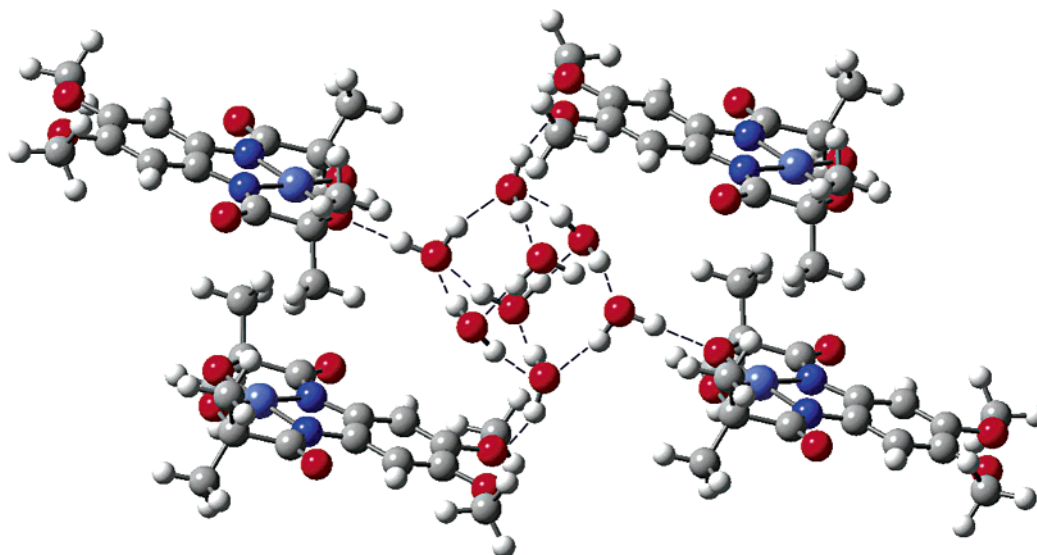


Figure 6. Section of the crystal structure of the (H₂O)₈/host system that shows the cubic (H₂O)₈ cluster anchored to four [A][−] units of the organometallic framework. Colors are as follows: gray, carbon; red, oxygen; dark blue, nitrogen; white, hydrogen; and light blue, cobalt.

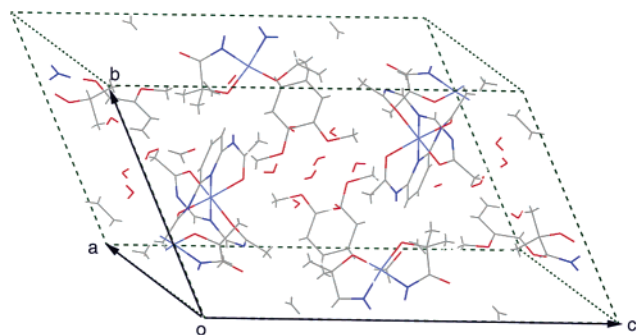


Figure 7. Section of the crystal structure of the $(\text{H}_2\text{O})_8/\text{host}$ system showing the a -, b -, and c -axes. Angles α , β , and γ refer to angles between the c - and b -axes, the a and c -axes, and the a - and b -axes, respectively.

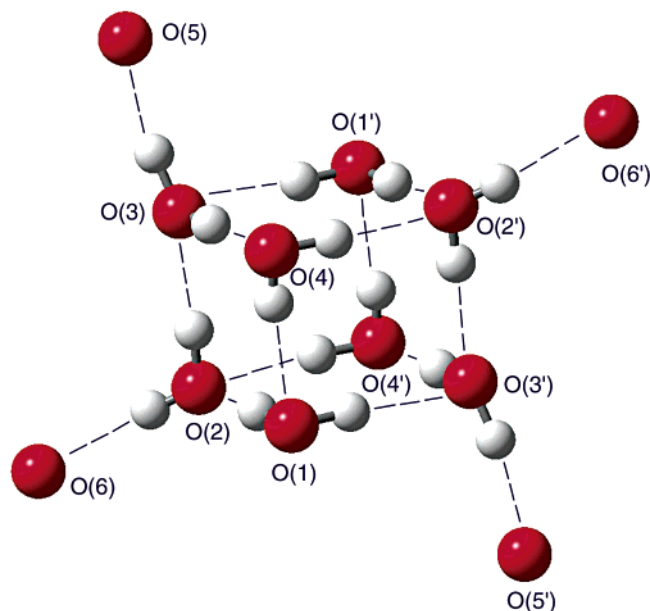


Figure 8. C_i -symmetry $(\text{H}_2\text{O})_8$ cluster hydrogen-bonded to the O atoms of the $[\text{A}]^-$ units.

In the case of the $(\text{H}_2\text{O})_6/\text{host}$ system, the presence of a stable dimensional chain of fused water hexamers encapsulated in the channel systems of $(\text{H}_2\text{O})_6/\text{host}$ was verified. However, the calculated lattice constant a of the crystal is appreciably larger than the measured value. The calculations confirm the existence of stable cubic octameric water clusters with C_i symmetry encapsulated in the cavities of the $(\text{H}_2\text{O})_8/\text{host}$ system. Again, some of the lattice constants differ appreciably from the experimental values. The deviations of the calculated structures from experiment are attributed to the failure of the DFT method used to describe long-range dispersion interactions adequately.

Acknowledgment. This work was supported by a grant from the National Science Foundation. The plane-wave DFT calculations were performed on the TCS computer at the Pittsburgh Supercomputer Center. We thank J. Steckel for valuable discussions and R. Christie for performing the LMP2 calculations.

References and Notes

- Xantheas, S. S.; Dunning, T. H. *J. Chem. Phys.* **1993**, *99*, 8774.
- Xantheas, S. S. *J. Chem. Phys.* **1994**, *100*, 7523. (c) Xantheas, S. S. *Chem. Phys.* **2000**, *258*, 225. (d) Xantheas, S. S.; Burnham, C. J.; Harrison, R. J. *J. Chem. Phys.* **2002**, *116*, 1493.
- Lee, H. M.; Suh, S. B.; Lee, J. Y.; Tarakeshar, P.; Kim, K. S. *J. Chem. Phys.* **2000**, *112*, 9759.
- Tissander, M. D.; Singer, S. S.; Coe, J. V. *J. Phys. Chem. A* **2000**, *104*, 752.
- Liu, K.; Brown, M. G.; Carter, C.; Saykally, R. J.; Gregory, J. K.; Clary, D. C. *Nature* **1996**, *381*, 501.
- Gruenloh, C. J.; Carney, J. R.; Arrington, C. A.; Zwier, T. S.; Fredericks, S. Y.; Jordan, K. D. *Science* **1997**, *276*, 1678. (b) Tsai, C. J.; Jordan, K. D. *J. Phys. Chem.* **1993**, *97*, 5208. (c) Pedulla, J. M.; Kim, K.; Jordan, K. D. *Chem. Phys. Lett.* **1998**, *291*, 78.
- Wales, D. J. In *Encyclopedia of Computational Chemistry*; Schleyer, P. v. R., Allinger, N. L., Clark, T., Gasteiger, J., Kollman, P. A., Schaefer, H. F., III, Schreiner, P. R., Eds.; Wiley: New York, 1998.
- Wales, D. J.; Hodges, M. P. *Chem. Phys. Lett.* **1998**, *286*, 65.
- Nauta, K.; Miller, R. E. *Science* **2000**, *287*, 293.
- Müller-Dethlefs, K.; Hobza, P. *Chem. Rev.* **2000**, *100*, 143.
- Ugalde, J. M.; Alkorta, I.; Elguero, J. *Angew. Chem.* **2000**, *112*, 733.
- Ugalde, J. M.; Alkorta, I.; Elguero, J. *Angew. Chem., Int. Ed.* **2000**, *39*, 717.
- Keutsch, F. N.; Saykally, R. J. *Proc. Natl. Acad. Sci.* **2001**, *98*, 10533.
- Barbour, L. J.; Orr, G. W.; Atwood, J. L. *Nature* **1998**, *393*, 671.
- Barbour, L. J.; Orr, G. W.; Atwood, J. L. *Chem. Commun.* **2000**, 859.
- Blanton, W. B.; Gordon-Wylie, S. W.; Clark, G. R.; Jordan, K. D.; Wood, J. T.; Geiser, U.; Collins, T. J. *J. Am. Chem. Soc.* **1999**, *121*, 3351.
- Custelcean, R.; Afloroaei, C.; Vlassa, M.; Polverejan, M. *Angew. Chem., Int. Ed.* **2000**, *39*, 3094.
- Atwood, J. L.; Barbour, L. J.; Ness, T. J.; Raston, C. L.; Raston, P. L. *J. Am. Chem. Soc.* **2001**, *7192*, 2001.
- Foces-Foces, C.; Cano, F. H.; Martinez-Ripoll, M.; Faure, R.; Roussel, C.; Claramunt, R. M.; Lopez, C.; Sanz, D.; Elguero, J. *Tetrahedron: Asymmetry* **1990**, *1*, 65.
- Collins, T. A., personal communication.
- Kristyan, S.; Pulay, P. *Chem. Phys. Lett.* **1994**, *225*, 280.
- Kresse, G.; Furthmüller, J. *Phys. Rev. B* **1996**, *54*, 11169. (b) Kresse, G.; Hafner, J. *Phys. Rev. B* **1994**, *49*, 4521.
- Vanderbilt, D. H. *Phys. Rev. B* **1990**, *41*, 7892. (b) Kresse, G.; Hafner, J. *J. Phys. Condens. Matter* **1994**, *6*, 8245.
- Perdew, J. P.; Wang, Y. *Phys. Rev. B* **1986**, *33*, 8800. (b) Perdew, J. P.; Chevary, J. A.; Vosko, S. H.; Jackson, K. A.; Pederson, M.; Singh, D. J.; Fiolhais, C. *Phys. Rev. B* **1992**, *46*, 6671.
- Tsuzuki, S.; Lüthi, H. P. *J. Chem. Phys.* **2001**, *114*, 3949.
- Computed values for the lattice parameters of $[\text{C}] \cdot (\text{H}_2\text{O})_6$ are $a = 8.3694 \text{ \AA}$, $b = 12.4450 \text{ \AA}$, $c = 14.5124 \text{ \AA}$, $\alpha = 81.895^\circ$, $\beta = 81.204^\circ$, $\gamma = 77.610^\circ$, and $V = 1449.8 \text{ \AA}^3$. The corresponding X-ray values are $a = 7.4737 \text{ \AA}$, $b = 12.5474 \text{ \AA}$, $c = 14.5261 \text{ \AA}$, $\alpha = 82.315^\circ$, $\beta = 84.305^\circ$, $\gamma = 80.020^\circ$, and $V = 1325.5 \text{ \AA}^3$.
- Eisenberg, D.; Kauzmann, W. *The Structure and Properties of Water*; Oxford University Press: Oxford, 1969.
- Dunning, T. H., Jr. *J. Chem. Phys.* **1989**, *90*, 1007. (b) Kendall, R. A.; Dunning, T. H., Jr.; Harrison, R. J. *ibid.* **1992**, *96*, 6796.
- Xantheas, S. S. *J. Chem. Phys.* **1995**, *102*, 4505.
- Frisch, M. J.; Trucks, G. W.; Schlegel, H. B.; Scuseria, G. E.; Robb, M. A.; Cheeseman, J. R.; Montgomery, J. A., Jr.; Vreven, T.; Kudin, K. N.; Burant, J. C.; Millam, J. M.; Iyengar, S. S.; Tomasi, J.; Barone, V.; Mennucci, B.; Cossi, M.; Scalmani, G.; Rega, N.; Petersson, G. A.; Nakatsuji, H.; Hada, M.; Ehara, M.; Toyota, K.; Fukuda, R.; Hasegawa, J.; Ishida, M.; Nakajima, T.; Honda, Y.; Kitao, O.; Nakai, H.; Klene, M.; Li, X.; Knox, J. E.; Hratchian, H. P.; Cross, J. B.; Adamo, C.; Jaramillo, J.; Gomperts, R.; Stratmann, R. E.; Yazyev, O.; Austin, A. J.; Cammi, R.; Pomelli, C.; Ochterski, J. W.; Ayala, P. Y.; Morokuma, K.; Voth, G. A.; Salvador, P.; Dannenberg, J. J.; Zakrzewski, V. G.; Dapprich, S.; Daniels, A. D.; Strain, M. C.; Farkas, O.; Malick, D. K.; Rabuck, A. D.; Raghavachari, K.; Foresman, J. B.; Ortiz, J. V.; Cui, Q.; Baboul, A. G.; Clifford, S.; Cioslowski, J.; Stefanov, B. B.; Liu, G.; Liashenko, A.; Piskorz, P.; Komaromi, I.; Martin, R. L.; Fox, D. J.; Keith, T.; Al-Laham, M. A.; Peng, C. Y.; Nanayakkara, A.; Challacombe, M.; Gill, P. M. W.; Johnson, B.; Chen, W.; Wong, M. W.; Gonzalez, C.; Pople, J. A. *Gaussian 03*, Revision A.1, Gaussian, Inc., Pittsburgh, PA, 2003.
- Pulay, P. *Chem. Phys. Lett.* **1983**, *100*, 151. (b) Saebø, S.; Pulay, P. *Annu. Rev. Phys. Chem.* **1993**, *44*, 213. (c) Saebø, S.; Tong, W.; Pulay, P. *J. Chem. Phys.* **1993**, *98*, 2170. (d) Hampel, C.; Werner, H.-J. *J. Chem. Phys.* **1996**, *104*, 6286. (e) Schütz, M.; Rauhut, G.; Werner, H.-J. *J. Chem. Phys.* **1998**, *102*, 5997.
- Jaguar, Version 4.2; Schrödinger, Inc.: Portland, OR, 2000.
- Computed values for the lattice parameters of $[\text{A}_2\text{B}](\text{H}_2\text{O})_8$ are $a = 14.1634 \text{ \AA}$, $b = 13.4535 \text{ \AA}$, $c = 21.5251 \text{ \AA}$, $\alpha = 114.852^\circ$, $\beta = 116.285^\circ$, $\gamma = 63.666^\circ$, and $V = 3165.4 \text{ \AA}^3$. The corresponding X-ray values are $a = b = 13.3585 \text{ \AA}$, $c = 21.9352 \text{ \AA}$, $\alpha = \beta = 113.175^\circ$, $\gamma = 66.886^\circ$, and $V = 3174.6 \text{ \AA}^3$.